Hopper Flows

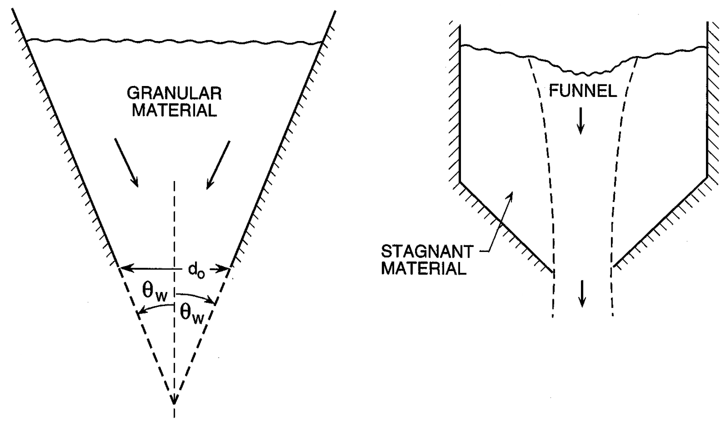

Figure 1: Some hopper geometries and notation. Left: a mass flow hopper. Right: funnel flow.

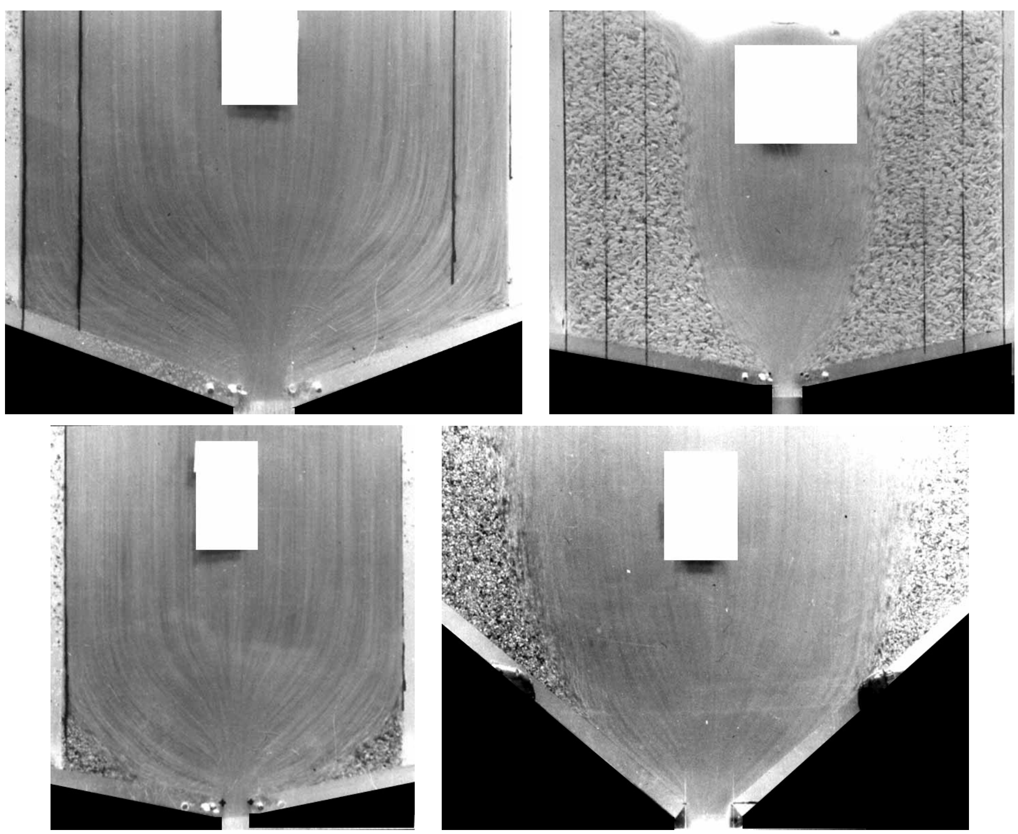

Figure 2: Long exposure photographs of typical granular flows in hoppers showing the streamlines in the flowing material. Top left: flow of sand without stagnant regions ($H/W = 3.3$). Top right: a funnel flow of rice. Bottom left: flow of sand with stagnant corners ($H/W = 1.6$). Bottom right: funnel flow of sand ($H/W = 1.16$). From Nguyen *et al.*(1980).

Two of the principal flow patterns that occur in conical or planar (two-dimensional) hoppers are sketched in Figure 1. Funnel flows are of considerable practical interest (see, for example, Jenike 1964, Johanson and Colijin 1964) and a substantial literature exists for the heuristic determination of the conditions under which they occur. One interpretation of funnel flow is that the stress state within the funnel is sufficient to allow dilation of the material and therefore flow whereas the surrounding stagnant material has a stress state in which the solids fraction remains above the critical. It should be possible to generate computer simulations of these complex flows that predict the boundaries between the shearing and non-shearing regions in a granular flow. However, it is clear that some of the experimentally observed flows are even more complex than implied by the above description. With some materials the flow can become quite unsteady; for example, Lee *et al.* (1974) observed the flow in a planar hopper to oscillate from side to side with the alternating formation of yield zones within the material.

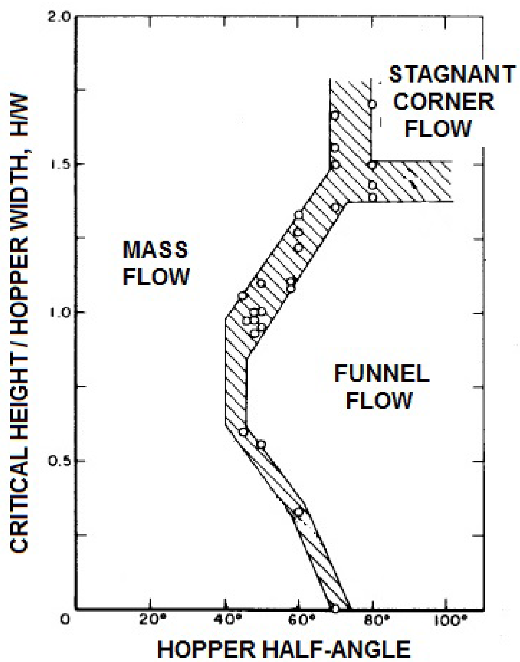

Figure 3: Flow regime map for sand in a planar hopper of width, $W = 15.24cm$, as a function of the material height in the hopper, H, and the hopper half-angle. From Nguyen *et al.* (1980).

Nguyen *et al.* (1980) used long exposure photographs to visualize the flows in planar hoppers of various half-angles for a range of material height, H, in the hoppers. Specifically, they investigated the conditions under which planar hoppers produce mass flow or funnel flow. Figure 3 is an example of their findings, in this case for sand (the results are qualitatively similar for glass beads and other granular materials) in a planar hopper of width, $W = 15.24cm$. Stagnant corner flow refers to a flow regime similar to that of Figure 2 (bottom left). Mass flow (Figure 2 (top left)) prevails for almost all material heights in the hopper, H, when the half-angle is less than about 50°. In contrast funnel flow (Figure 2 (top right) and Figure 2 (bottom right)) prevails for greater half-angles (or for more frictional materials) though it may also be suppressed when the material height in the hopper becomes large; then the flow pattern tends toward the stagnant corner flow typified by Figure 2 (bottom left) or to the mass flow configuration. Thus funnel flow may develop during the last phase of discharge when earlier mass flow prevailed (see Figure 4).

Mohr-Coulomb models have had some modest success in predicting the mass flow rates from planar and conical hoppers operating in the mass flow regime. Savage (1965, 1967), Morrison and Richmond (1976), Brennen and Pearce (1978), Nguyen *et al.*(1979), and others utilized Mohr-Coulomb models (and other

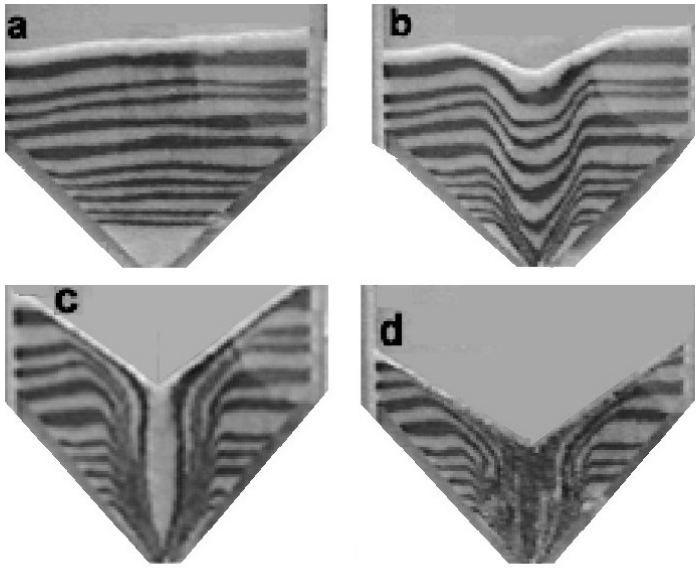

Figure 4: Photographs of funnel flow at four moments in time during discharge from a two-dimensional hopper. From Hunt *et al.* (1999).

variants) to find approximate analytical solutions for the flows in hoppers, both conical and planar hoppers. In narrow *mass flow* hoppers with small opening angles, θ_w, these solutions yield flow rates that agree well with the experimentally measured values for various values of θ_w, various internal friction angles and wall friction angles. An example of the comparison of calculated and experimental flow rates is included in Figure 5. These methods also appear to yield roughly the right wall stress distributions. In addition note

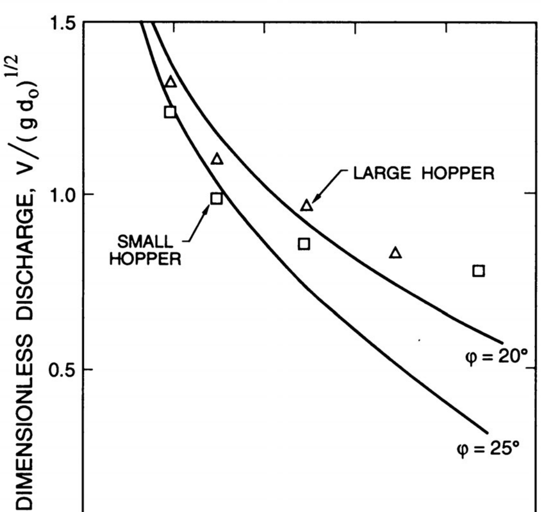

Figure 5: Dimensionless discharge, $V/(gd_o)^{\frac{1}{2}}$ (d_o is the opening width and V is the volume-averaged opening velocity), for flows in conical hoppers of various hopper opening angles, θ_w. Experimental data for the flows of glass beads (internal friction angle, $\phi = 25^o$, wall friction angle of 15^o) in two sizes of hopper are compared with the Mohr-Coulomb-Jenike-Shield calculations of Nguyen *et al.*(1979) using internal friction angles of 20° and 25°.

that both experimentally and theoretically the flow rate becomes independent of the height of material in the hopper once that height exceeds a few opening diameters; this result was explored by Janssen (1895) in one of the earliest papers dealing with granular flow.